

Article

# Parameter Identification of Electrochemical Model for Vehicular Lithium-Ion Battery Based on Particle Swarm Optimization

Xiao Yang <sup>1</sup>, Long Chen <sup>1,2</sup>, Xing Xu <sup>1,2,\*</sup>, Wei Wang <sup>1</sup>, Qiling Xu <sup>1</sup>, Yuzhen Lin <sup>1</sup> and Zhiguang Zhou <sup>3</sup>

<sup>1</sup> School of Automotive and Traffic Engineering, Jiangsu University, Zhenjiang 212013, Jiangsu, China; 2211504035@stmail.ujs.edu.cn (X.Y.); chenlong@ujs.edu.cn (L.C.); wangwei17@saicmotor.com (W.W.); 2221604075@stmail.ujs.edu.cn (Q.X.); 2211704011@stmail.ujs.edu.cn (Y.L.)

<sup>2</sup> Automotive Engineering Research Institute, Jiangsu University, Zhenjiang 212013, Jiangsu, China

<sup>3</sup> New Energy Development Department Powertrain Technology Center, Chery Automobile Co., Ltd., Wuhu 241009, Anhui, China; zhoughuiguang@mychery.com

\* Correspondence: xuxing@mail.ujs.edu.cn

Received: 23 October 2017; Accepted: 7 November 2017; Published: 9 November 2017

**Abstract:** The dynamic characteristics of power batteries directly affect the performance of electric vehicles, and the mathematical model is the basis for the design of a battery management system (BMS). Based on the electrode-averaged model of a lithium-ion battery, in view of the solid phase lithium-ion diffusion equation, the electrochemical model is simplified through the finite difference method. By analyzing the characteristics of the model and the type of parameters, the solid state diffusion kinetics are separated, and then the cascade parameter identifications are implemented with Particle Swarm Optimization. Eventually, the validity of the electrochemical model and the accuracy of model parameters are verified through 0.2–2 C multi-rates battery discharge tests of cell and road simulation tests of a micro pure electric vehicle under New European Driving Cycle (NEDC) conditions. The results show that the estimated parameters can guarantee the output accuracy. In the test of cell, the voltage deviation of discharge is generally less than 0.1 V except the end; in road simulation test, the output is close to the actual value at low speed with the error around  $\pm 0.03$  V, and at high speed around  $\pm 0.08$  V.

**Keywords:** lithium-ion battery; electrochemical model; particle swarm optimization; parameter identification

## 1. Introduction

Recently, due to advantages of high energy density, high output power, long life, zero pollution, and wide operating temperature range, lithium-ion batteries have been attached great importance to new energy automotive industry with being the preferred choice. However, the battery applied to automobile is required not only can provide large energy and power, but also ensure its safety and reliable operation, and the performance will change with time, explosion may even occur in overcharge or harsh conditions. So, real-time monitoring system of on-board power battery is essential.

In management of vehicle power batteries, an exact battery model is usually required to estimate the state accurately. At present, simple equivalent circuit model (ECM) is widely used because of its simple structure, rapid calculation, and relatively good battery state of charge (SOC) prediction capability [1], including classic Rint [1], Resistance-Capacitance Circuits (RC) [1], Thevenin [2], and the Partnership for a New Generation of Vehicles (PNGV) [3] models. A lot of follow-up research has been carried out on the equivalent circuit model. Z Gao, et al. designed and implemented a smart lithium-ion

battery system with real-time fault diagnosis capability for electric vehicles to ensure battery safety and performance [4]. They also put forward an integrated equivalent circuit and thermal model of a temperature-dependent  $\text{LiFePO}_4$  battery in an actual embedded application, which applied a cell balancing strategy to balance the SOC of each cell to increase the lifespan of the battery [5]. However, the parameters of model cannot correspond to actual physical quantities, and the prediction accuracy of battery state depends largely on the previous experimental data. Unlike ECM, an electrochemical model is established using the physical chemistry and electrochemistry theory, which can reflect the internal reaction mechanism to make an accurate prediction of internal basic state, such as the concentration of lithium ion, the potential in electrolyte and solid electrode materials. But owing complex structure, numerous parameters, and highly nonlinear, it is hard to meet the operational speed of real-time control system. Therefore, model simplification must be carried out first.

So far, literatures on electrochemical model of battery are quite extensive. Newman and Tiedemann presented the first electrochemical approach to porous electrodes modeling for battery applications [6]. Then, Doyle et al. proposed lithium anode/solid polymer separator/insertion cathode cell model, a full-order model, based on concentrated solution theory [7]. This model was later widely cited, and many electrochemical models were simplified on the basis of it. Such as the micro-macroscopic coupled model, which introduced by Wang et al. in 1998 [8] with a great deal of research on battery state estimation and energy management [9,10]. In fact, it was presented for Ni-MH batteries at the beginning [11]. Then, it was expanded to lithium-ion batteries [12], where the thermal behavior was also described. In addition, Chaturvedi and Klein [13] established a simpler single particle model (SPM) by assuming the solid diffusion of electrode to be the diffusion within a single spherical particle. Similarly, the average-electrode model, studied by Di Domenico et al. [14,15], replaces the specific distribution of Li-ion concentration in electrode with the average concentration, greatly pushing the complexity into smaller. Both of them have high accuracy at low to moderate operating rate, but the latter has higher order with the important diffusion kinetic characteristics in the solid particles retained. However, these models still have higher complexity than the circuit model, which limits their application in the control system. Therefore, the further reduction is also the focus. Smith and Wang reduced the diffusion dynamics by using the residue grouping [16]. Lee and Filipi obtained the ideal non-uniform discrete mode by Sequential Quadratic Programming (SQP), and reduced the order of the state space model while guaranteeing the accuracy [17]. In recent years, Zou, Manzie, and Nesic are committed to the simplification techniques for Partial Differential Equation (PDE)-based Li-ion battery models [18], and have developed a framework for battery model simplification starting from an initial high-order physics-based model [19].

From the introduction above, the research of the equivalent circuit model has been basically perfected, and the corresponding battery management technology is generally based on the circuit model. But the study of electrochemical models is still in its infancy, and rising stage. Therefore, the research on the electrochemical model of lithium ion and its model reduction method can also help to promote the application of electrochemical theory in the development of battery management technology.

In addition, the parameters of the model need to be identified after the model is built. For the equivalent circuit model, pulse charging and discharging experiment can be used to perform offline parameter identification [20]. Many scholars adopt the pulse test at different temperature, current rates, and SOC to improve the accuracy [21,22]. But in practice, the parameters are constantly changing, so the most accurate battery model can only be obtained by real-time online identification. Currently, improved least squares method or extended Kalman filter algorithm are the most widely used. As for the electrochemical model, offline identification combined with some intelligent algorithms is adopted more as a result of numerous electrochemical and complex identification methods.

In this paper, the average electrode model of lithium-ion battery combined with the uniformly discrete finite difference method can firstly reduce the complexity of the electrochemical model. Secondly, the electrochemical model characteristics and parameter types of Li-ion batteries are analyzed.

The solid phase lithium-ion diffusion kinetics are separated, and the parameters are identified by PSO. Finally, the accuracy of the parameters was verified by the multi-rate discharge test of single cells and the NEDC cycle experiment of vehicle.

## 2. Electrochemical Model of Lithium Ion Battery

### 2.1. Average Electrode Model

Di Domenico et al. proposed the average electrode model of the battery in References [14,15], which was simplified on the basis of the micro-macroscopic coupled battery model advanced in the literature [8]. In order to reduce the complexity of the model, the electrolyte concentration in the average electrode model is considered as a constant value, and the electrode dynamics characteristic of the  $X$  axis in the cross section is considered only. This approximation (depicted in Figure 1) consists of three domains—the positive composite electrode (consist of  $\text{Li}_y\text{Mn}_2\text{O}_4$ ,  $\text{Li}_y\text{CoO}_2$ ,  $\text{Li}_y\text{NiO}_2$ , or some combination of metal oxides), separator, and negative composite electrode (with  $\text{Li}_x\text{C}_6$  active material). During the charging and discharging, the lithium ion is embedded and removed between the positive and negative electrodes.

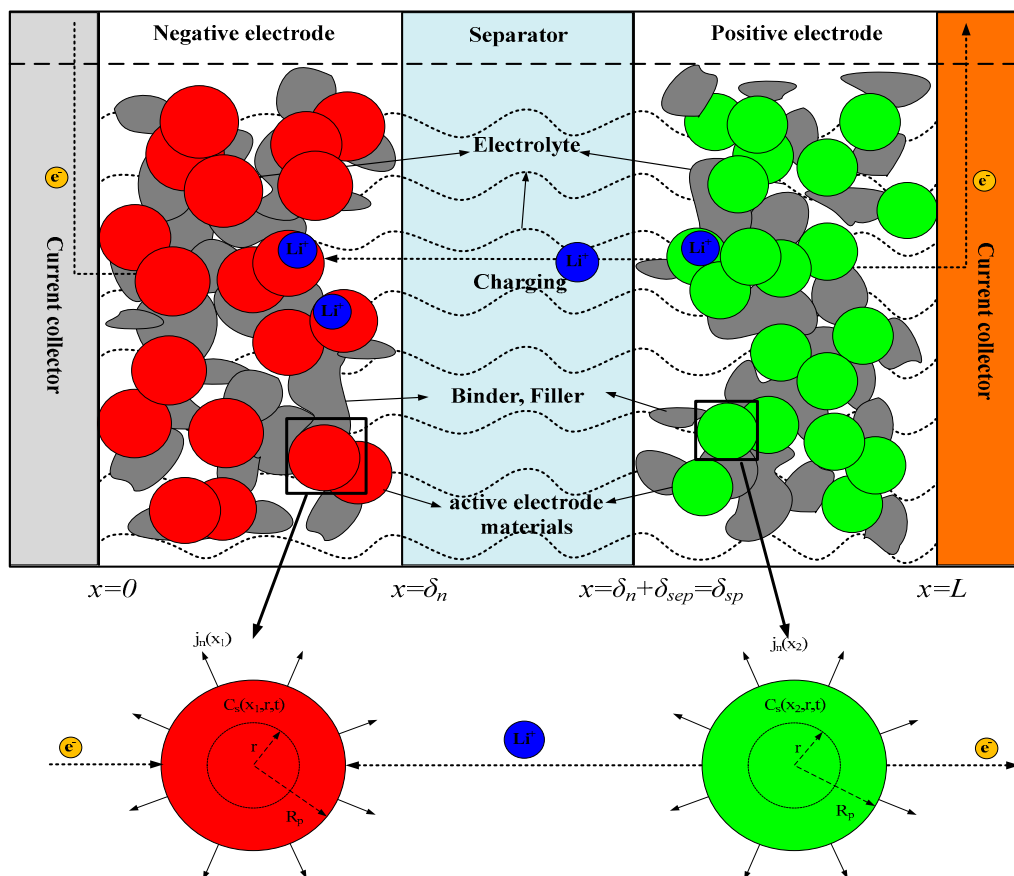


**Figure 1.** Schematic macroscopic ( $x$ -direction) cell model with coupled microscopic ( $r$ -direction) solid diffusion model.

The electrochemical model is actually based on a series of differential algebraic equations describing the internal potential and ion diffusion. The specific equations and boundary conditions are shown in Table 1 [23], which an ideal model can be constructed from, and the detailed derivation process can be referenced to [14].

**Table 1.** Equations of electrochemical model for Li-ion batteries.

Kinetic Equations		Boundary Condition
Liquid potential	$\frac{\partial \phi_e(x,t)}{\partial x} = -\frac{i_e(x,t)}{\kappa^{eff}}$ $\frac{\partial i_e(x,t)}{\partial x} = j^{Li}$	$\left. \frac{\partial \phi_e}{\partial x} \right _{x=0, x=L} = 0$ $\left. \frac{\partial \phi_e}{\partial x} \right _{x=\delta_n, x=\delta_{sp}} = -\frac{I}{A\kappa^{eff}}$
Solid potential	$\frac{\partial \phi_s(x,t)}{\partial x} = -\frac{i_s(x,t)}{\sigma^{eff}}$ $\frac{\partial i_s(x,t)}{\partial x} = -j^{Li}$	$\left. \frac{\partial \phi_s}{\partial x} \right _{x=\delta_n, x=\delta_{sp}} = 0$ $\left. \frac{\partial \phi_s}{\partial x} \right _{x=0, x=L} = -\frac{I}{A\sigma^{eff}}$
Lithium-ion concentration in Solid phase	$\frac{\partial c_s(x,r,t)}{\partial t} = \frac{1}{r^2} \frac{\partial}{\partial r} \left( D_s r^2 \frac{\partial c_s(x,r,t)}{\partial r} \right)$	$\left. \frac{\partial c_s}{\partial r} \right _{r=R_s} = -\frac{j^{Li}}{a_s F D_s}, \left. \frac{\partial c_s}{\partial r} \right _{r=0} = 0$
Butler Volmer	$j_n(x,t) = \frac{i_0(x,t)}{F} \left[ \exp\left(\frac{\alpha_a F}{RT} \eta_s(x,t)\right) - \exp\left(\frac{-\alpha_c F}{RT} \eta_s(x,t)\right) \right]$ $\eta_s(x,t) = \Phi_s(x,t) - \Phi_e(x,t) - \mu(c_{ss}(x,t)) - FR_f j_n(x,t)$ <p>where: <math>i_0(x,t) = r_{eff} c_e(x,t)^{\alpha_a} * (c_{s,max} - c_{ss}(x,t))^{\alpha_n} c_{ss}(x,t)^{\alpha_c}</math>  <math>c_{ss}(x,t) \equiv c_s(x, R_s, t)</math></p>	
Battery terminal voltage	$V(t) = \eta(L,t) - \eta(0,t) + (\phi_e(L,t) - \phi_e(0,t)) + (U_p(c_{se}(L,t)) - U_n(c_{se}(0,t))) - R_f I$	

First of all, according to the idea of average electrode, the negative current density  $j^{Li}$  of Butler Volmer is integrated in the direction of  $X$ , and combined with the liquid phase current density at the boundary, and the average value  $\bar{j}_n^{Li}$  can be deduced.

$$\bar{j}_n^{Li}(t)\delta = \int_0^\delta j^{Li}(x',t)dx' = i_e(\delta_n,t) - i_e(0,t) = \frac{I}{A} - 0 \quad (1)$$

In formula:  $\delta_n$  is negative electrode thickness.

Then, the terminal voltage can be simplified as a polynomial expressed by the average values at the positive and negative electrodes in accordance with the boundary conditions in the table. The specific derivation process can be referred to [14], and the voltage output Equation is:

$$V(t) = \bar{\eta}_p(t) - \bar{\eta}_n(t) + (\bar{\varphi}_{e,p}(t) - \bar{\varphi}_{e,n}(t)) + (U_p(\bar{c}_{se,p}(t)) - U_n(\bar{c}_{se,n}(t))) - R_f I \quad (2)$$

Finally, according to the boundary conditions, the solid-liquid phase potential, the Butler Volmer kinetic equation, and continuity of physical quantities at the model boundary in Table 1. The terminal voltage of battery can be further written as a function of load current and the average solid concentration lithium.

$$V(t) = \frac{RT}{\alpha_a F} \ln \frac{\bar{\zeta}_n + \sqrt{\bar{\zeta}_n^2 + 1}}{\bar{\zeta}_p + \sqrt{\bar{\zeta}_p^2 + 1}} - \frac{I}{2A} \left( \frac{\delta_n}{\kappa^{eff}} + 2 \frac{\delta_{sep}}{\kappa^{eff}} + \frac{\delta_p}{\kappa^{eff}} \right) + (U_p(\bar{c}_{se,p}(t)) - U_n(\bar{c}_{se,n}(t))) - R_f I \quad (3)$$

In formula:  $\bar{\zeta}_n = \frac{\bar{j}_n^{Li}(t)}{2aj_0}$ ,  $\bar{\zeta}_p = \frac{\bar{j}_p^{Li}(t)}{2aj_0}$ .

The lithium battery system is a strongly nonlinear distributed dynamical system with strong coupling. After the simplification above, the model can be represented by lithium-ion concentration in solid phase in the Table 1 and (3). But it is difficult to solve directly for the partial differential equation, and further simplification is necessary. In addition, it can be seen from the Formula (3) that in order to obtain the battery terminal voltage, it is also essential to figure out the distribution of solid-phase concentration.



**Table 2.** Electrochemical model parameters of Li-ion battery.

Parameter	Performance Parameter	Structural Parameter	Constant Parameter		
Model parameters of average electrode for Li-ion battery	$E_{s,n}$	0.1~0.9	$R_{p,n}$ $1.5 \times 10^{-3} \sim 2.5 \times 10^{-3}$	$F$ 968,485	
	$E_{s,p}$	0.1~0.9	$R_{p,p}$ $5 \times 10^{-4} \sim 1.5 \times 10^{-3}$	$SOC_{ini}$ 1	
	$D_{s,n}$	$1 \times 10^{-11} \sim 1 \times 10^{-9}$	$L_n$ $2 \times 10^{-3} \sim 2 \times 10^{-2}$	$\theta_{n,0}$ 0.126	
	$D_{s,p}$	$1 \times 10^{-11} \sim 1 \times 10^{-9}$		$\theta_{p,0}$ 0.936	
	$C_{s,max,n}$	$1 \times 10^{-3} \sim 1 \times 10^{-2}$	$L_p$ $2 \times 10^{-3} \sim 2 \times 10^{-2}$	$\theta_{n,100}$ 0.676	
	$C_{s,max,p}$	$1 \times 10^{-3} \sim 1 \times 10^{-2}$		$\theta_{p,100}$ 0.442	
		$E_{e,sep}$	0.1~0.9	$T$ 298.15	
		$R_f$	0~200	$\alpha$ 0.5	
		$E_{e,n}$	0.1~0.9	$L_{sep}$ $1 \times 10^{-3} \sim 1 \times 10^{-2}$	$R$ 8.314
		$E_{e,p}$	0.1~0.9		
	$C_e$	$1 \times 10^{-3} \sim 1 \times 10^{-2}$			

The performance parameters are the main factors that determine battery charging and discharging performance, the same type also will change in different health conditions. In the future study of battery aging and health problems, some of the performance parameters can be paid close attention to. The structural parameters will not change significantly during use, and the consistency of batteries is basically the same. The constant parameters contain the basic electrochemical coefficients, constant parameters of lithium batteries, and some accessible parameters. Where,  $\theta_{p,100}$ ,  $\theta_{n,100}/\theta_{p,0}$ ,  $\theta_{n,0}$  indicate the positive and negative solid-phase lithium ion concentration in the full or empty state of battery. Since the concentration information in the battery is too difficult to obtain, the value in document [14] is referenced here. In addition, the positive and negative open circuit voltages affected by them are corresponding to the concentration of the solid phase lithium-ion in the electrodes, and whose curves are mostly fitted by the experimental data. It is found that these four parameters mentioned above only limit the range of concentration, therefore, the error of these parameters will have little influence on the accuracy of the model in this paper.

Furthermore, it should be emphasized that in the use of batteries, excessive charging and discharging must be strictly avoided, in the electrochemical model, the positive and negative solid phase lithium-ion concentration should be limited within the parameter range above according to the close relationship between the solid phase lithium-ion concentration and the SOC. The parameter identification of the solid phase lithium-ion diffusion in cell model can be carried out separately, which is not only helpful to ensure the battery running in normal state, but also beneficial to improve the workload, accuracy, complexity of the algorithm brought by one-time identification.

### 3.2. Particle Swarm Optimization

Particle Swarm Optimization (PSO), also called bird swarm foraging algorithm. It is an evolutionary computation technique developed by Kennedy and Eberhart in 1995 [23]. The algorithm was first inspired by the regularity of bird swarm activity, and then a simplified model was built using swarm intelligence. Particle swarm optimization algorithm based on the observation in animal behavior of cluster activities, information sharing makes the population movement from disorderly to orderly evolution in problem solving space by a group of individuals, so as to obtain the optimal solution. It means that the optimal solution is searched by iteration from the stochastic solution, and the quality of the solution is evaluated by fitness. In recent years, PSO has attracted the attention of academics for its advantages of easy implementation, high precision, fast convergence, and has demonstrated its superiority in solving practical problems. The specific algorithm steps are as follows:

- Step 1: Parameter setting

Determine some basic parameters based on the battery model, including the number of population sizes, the dimensions of a single particle, and the range of dimensions in operation, which can be defined according to the range of the cell parameters given in Table 2.

- Step 2: Initializing the particle swarm

Initialize Particle Swarm (population size is  $n$ ), including random locations and velocities. All set as [0–1] random numbers.

- Step 3: Calculate the fitness of each particle

In the algorithm, each dimension of a single particle represents a complete set of model parameters, and then  $n$  particles make up a population. The objective function is set to calculate the corresponding errors of each set of parameters with the fitness obtained accordingly.

- Step 4: Finding the individual optimum position ( $pbest$ )

For each particle, the current adaptation is compared with the adaptive value corresponding to its individual historical best position ( $pbest$ ). Then, the  $pbest$  will be updated with the current position if the current adaptation value is better.

- Step 5: Finding the global optimum position ( $gbest$ )

Similarly, compare the current fitness with the adaptation of the global optimum position ( $gbest$ ), and update the  $gbest$  with the current particle location if the current adaptation value is better.

- Step 6: Update the velocity and position of each particles

Update the velocity and position of the dimension  $d$  of the particle  $i$  according to Formulas (7) and (8):

$$v_{id}^k = wv_{id}^{k-1} + c_1r_1(pbest_{id} - x_{id}^{k-1}) + c_2r_2(pbest_d - x_{id}^{k-1}) \quad (7)$$

$$x_{id}^k = x_{id}^{k-1} + v_{id}^{k-1} \quad (8)$$

where  $v_{id}^k$  is the  $d$  dimensional component of the velocity vector of particle  $i$  in the  $k$  iteration and  $x_{id}^k$  is the position vector;  $c_1$ ,  $c_2$  is the acceleration constant, adjusting learning maximum step size;  $r_1$  and  $r_2$  are two random functions, in the range [0, 1] to increase search randomness;  $w$  is the inertia weight, a nonnegative number, which regulates the search range of solution space.

- Step 7: Loop iteration to algorithm terminates

Repeat the 3 to 6 steps above until the maximum iteration or the increment of the optimum fitness is less than a given threshold. The algorithm stops.

Because the electrochemical model studied in this paper is relatively complex, involving many parameters, particle swarm optimization (PSO) is exactly suitable for solving such problems. And according to the model structure and parameter division above, we can divide all the parameters into two parts and identify them in turn.

### 3.3. Identification of Parameters Related to Solid-Phase Lithium Ion Diffusion Kinetics

The solid-phase lithium ion diffusion kinetics of positive and negative electrodes plays a relatively independent but crucial role in the model, and the concentration of lithium ion can be received by solving the diffusion equation. The diffusion model of positive electrode can be established by the state space Equation (5) as shown in Figure 2.

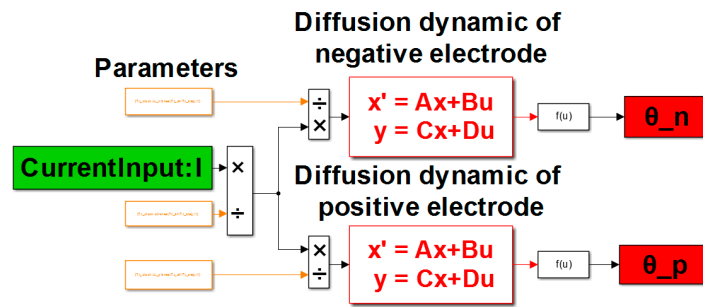


Figure 2. Solid phase lithium-ion diffusion kinetic model.

Write the parameter identification code based on the algorithm steps described above, the number of population size  $SwarmSize = 30$ , the dimension of a particle  $ParticleSize = 10$ , the inertia weight  $w = 0.7$ , acceleration constant  $c_1 = c_2 = 2$  and restriction factor  $a = 0.792$ . Perform 50 iterations.

In the algorithm, the individual evaluation index is the error function of the positive and negative solid-phase lithium ion concentration at the end of the discharge:

$$error(i) = abs(\theta_n - \theta_{n,0}) + abs(\theta_p - \theta_{p,0}) \tag{9}$$

where,  $\theta_p$  and  $\theta_n$  respectively indicates the concentration of solid-phase lithium ion at the end of discharge. On the one hand, the objective function can be used as a calculation index of individual fitness. On the other hand, it can avoid the dangerous state of excessive discharge in simulation.

The algorithm runs as shown in Figure 3. The error decreases gradually with the iterations. The error of the 50th generation is acceptable of 0.0034, and the final identification of parameters is shown in Table 3.

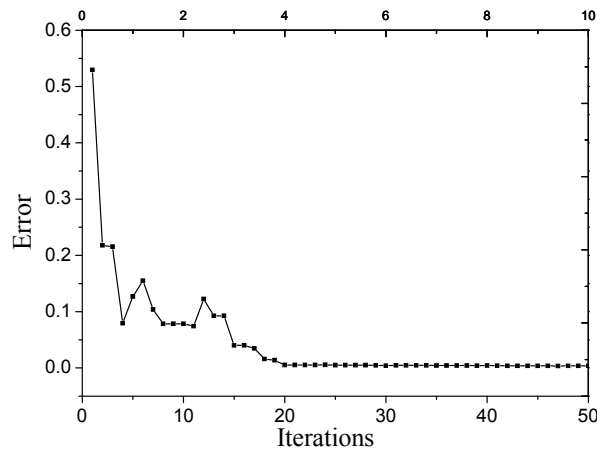


Figure 3. Optimal solution and performance tracking after 50 iterations.

Table 3. Identification results of kinetic parameters of solid-phase lithium ion diffusion.

Parameter	Value	Parameter	Value
$Es_n$	0.4638	$Es_p$	0.5186
$L_n$	0.0097	$L_p$	0.0119
$Ds_n$	$7.1908 \times 10^{-10}$	$Ds_p$	$1.7080 \times 10^{-10}$
$Rp_n$	0.0018	$Rp_p$	$5.8806 \times 10^{-4}$
$Csmax_n$	0.0091	$Csmax_p$	0.0075

### 3.4. Voltage Curve Fitting of Positive and Negative Electrodes

The battery terminal voltage is divided into four parts in the average electrode model, they are over potential, electrolyte-phase potential, electrode open circuit potential, and potential caused by internal resistance. The third part in Formula (2) is the battery positive and negative electrode open circuit potential, usually expressed as a function of the electrode solid-phase lithium ion concentration, which can be obtained by fitting experimental data. But the open circuit potentials will not be the same with different materials, the battery studied in this paper will be just chosen a ternary battery with the negative electrode material being  $\text{Li}_x\text{C}_6$ , the cathode material being  $\text{Li}(\text{NiCoMn})\text{O}_2$ . At present, there is little difference between the anode materials, but cathode materials have many kinds with different corresponding potential curves. Thus, the negative open circuit potential expression of this paper will refer to the polynomial in the literature [10], the positive expression can be got by fitting experimental data. The specific formula is as follows. The relation curve between the potential and the concentration is shown in Figures 4 and 5.

$$U^-(\theta_n) = 0.7222 + 0.1387 \times \theta_n + 0.029 \times \theta_n^{0.5} - 0.0172/\theta_n + 0.0019 \times \theta_n^{-1.5} + 0.2808 \times \exp(0.9 - 15 * \theta_n) - 0.7984 \times \exp(0.4465 \times \theta_n - 0.4108) \quad (10)$$

$$U^+(\theta_p) = -3336608 \times \theta_p^{10} + 2224336 \times \theta_p^9 - 66321816 \times \theta_p^8 + 116462170 \times \theta_p^7 - 133373853 \times \theta_p^6 + 104078116 \times \theta_p^5 - 56042493 \times \theta_p^4 + 20560010 \times \theta_p^3 - 4917875 \times \theta_p^2 + 692535 \times \theta_p - 43591.6828 \quad (11)$$

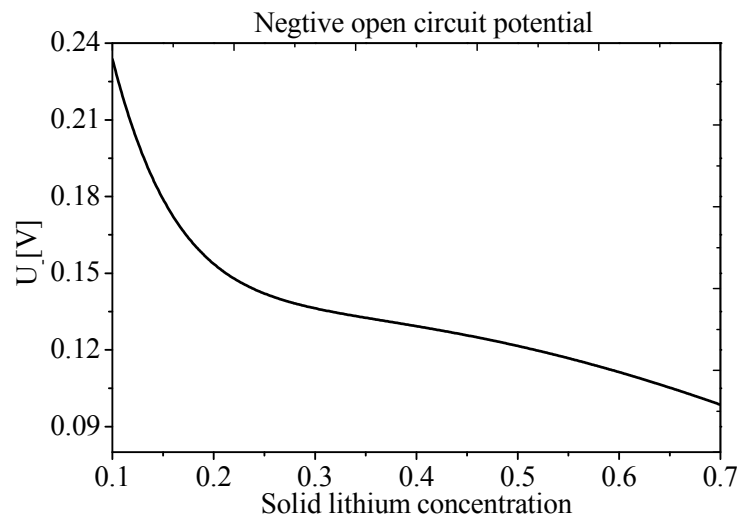


Figure 4. Negative open circuit potential.

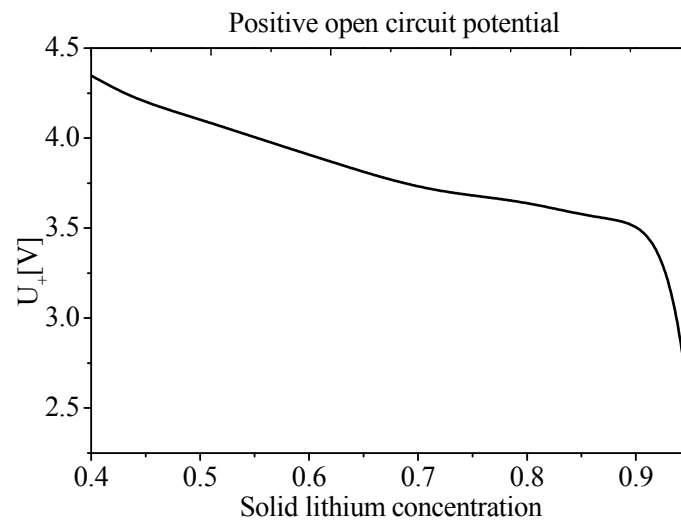


Figure 5. Positive open circuit potential.

### 3.5. Model Remaining Parameter Identification

The remaining parameters of the model can also be identified by particle swarm optimization. On the basis of the relevant parameters of the identified solid-phase diffusion kinetics, a complete battery average electrode model is established by Equations (10) and (12), as shown in Figure 6.

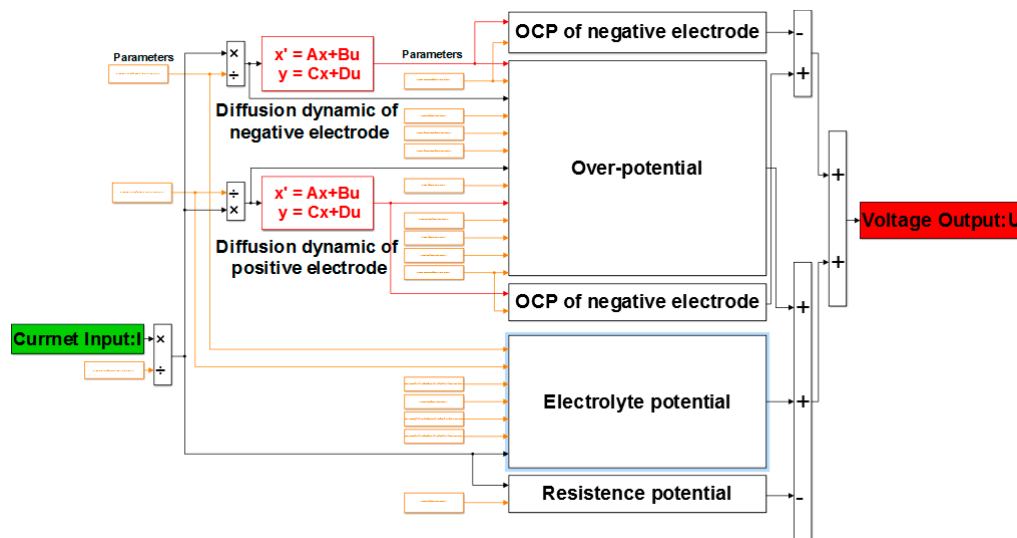


Figure 6. Average electrode model of lithium ion battery. OCP: open circuit potential.

The input of model is load current, and output is battery terminal voltage. According to the experimental data of battery, the identification code is written, and all the parameters can be received ultimately. Set the SwarmSize = 20, the ParticleSize = 6, other parameter settings are consistent with the previous ones to carry out 20 iterations. The individual evaluation index is the mean error function of the battery terminal voltage:

$$error(i) = avg(U\_experiment - U\_simulink) \tag{12}$$

Operation results as shown in Figure 7, the error of the 20th generation is 0.0040. And the identification results of the remaining 6 parameters are shown in Table 4.

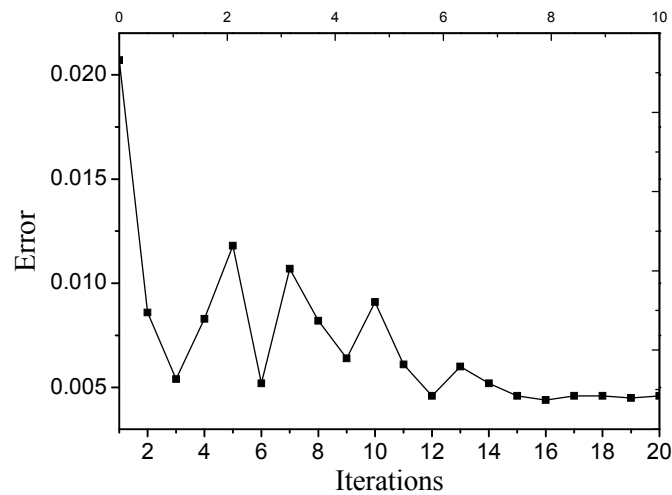


Figure 7. Optimal solution and performance tracking after 20 iterations.

Table 4. Identification results of model remaining parameters.

Parameter	Value	Parameter	Value
$Ee_{sep}$	0.4732	$R_f$	194.8967
$Ee_n$	0.6626	$Ee_p$	0.8812
$Ce$	0.0019	$L_{sep}$	0.0053

At this point, the 16 unknown parameters of the average electrode model are identified by two PSO algorithms with the error all in reasonable limits. The battery test used in parameter identification is 0.5 C discharge to the cut-off voltage 2.7 V under constant temperature and current, then hold 15 min. And in this test, the initial SOC is 100%, the ambient temperature is 25 °C. The voltage curve shown in Figure 8 indicates that the terminal voltage of the model output is basically consistent with the experimental data, which shows that the model parameters identified with PSO can meet the precision.

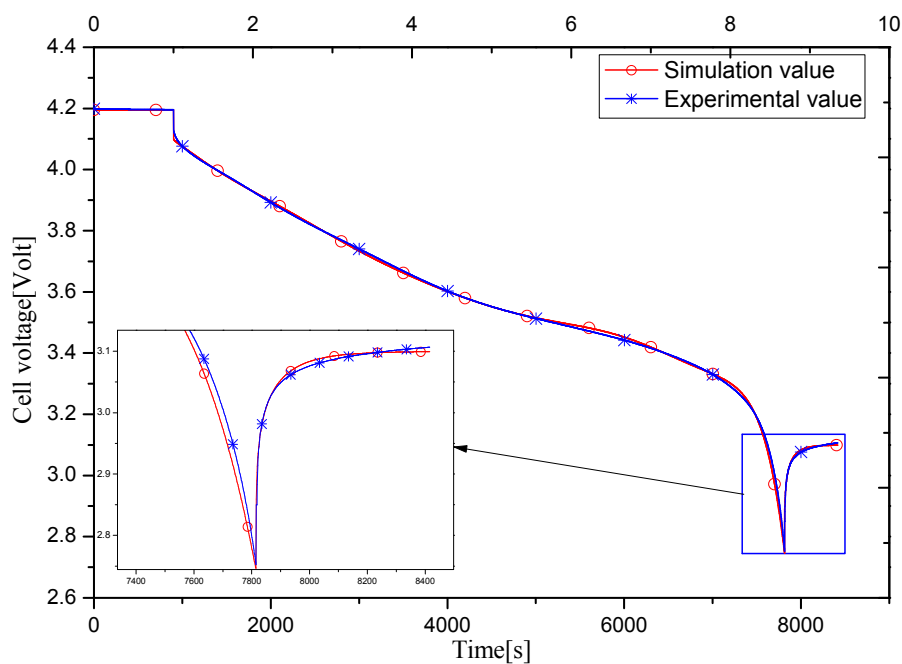
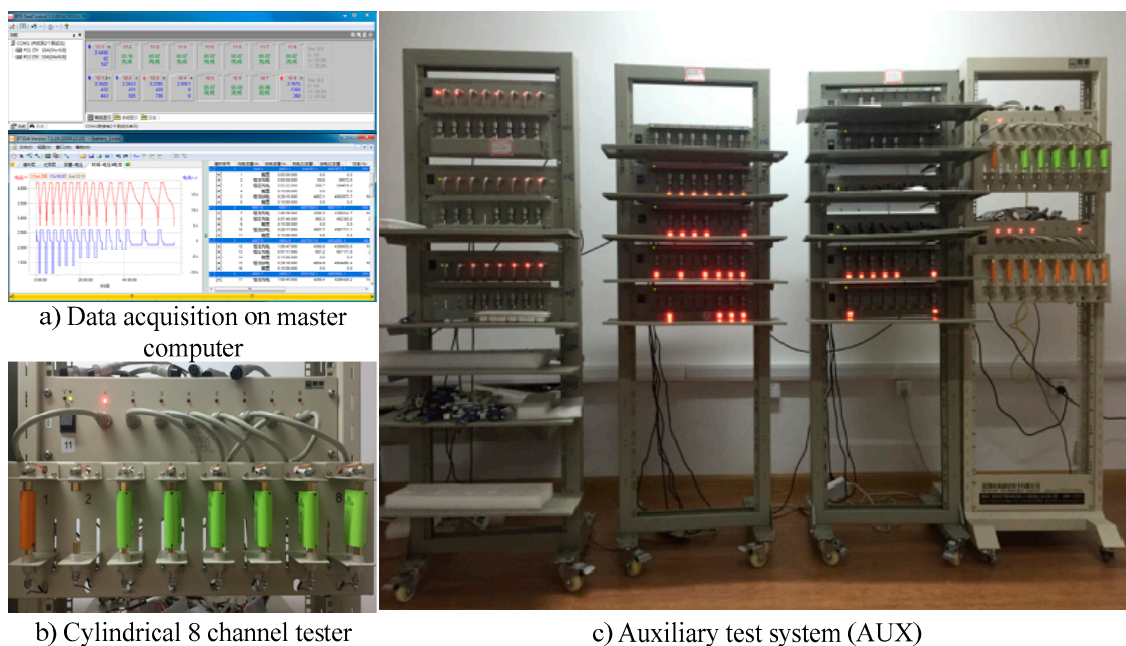


Figure 8. Comparison of experiment and simulation results of 0.5 C discharge.

#### 4. Simulation and Experimental Result

Based on the experimental data of 0.5 C discharge, the identification of all parameters of the battery electrochemical model is completed. The output voltage of the model has been found as essentially in agreement with the experimental value. In order to verify the accuracy and the validity, we use the NEWARE battery test system (BTS-5V/10A) shown in Figure 9 to test the battery discharge at different rates. NEWARE battery test system is the equipment that can realize the comprehensive performance test of various rechargeable batteries with different shapes. In addition, the system has the advantages of a stable and reliable hardware system, computer monitoring, convenient operation, clear results, and accuracy of 0.1%. The experiments consisted of five groups of constant current discharge tests, (0.2 C, 0.5 C, 1 C, 1.5 C and 2 C), and the initial SOC was set as 100%, the ambient temperature will be maintained at 25 °C. The test will be terminated when the discharge cut-off voltage reaches 2.7 V and then hold 15 min.



**Figure 9.** NEWARE battery test system.

The final experimental and simulation results are shown in Figure 10. It is a 0.5 C battery discharge test performed to identify model parameters, therefore, in the small current discharge of 0.2 C and 0.5 C, the model voltage is basically the same as the actual one. Moreover, the amount of electricity is released the same in experiment and simulation, the average error of voltage is 0.0106 V and 0.004 V, not more than 0.1 V.

It can be seen that the output voltage error of model, increases with the increment of current. The discharge curves of 1 C, 1.5 C, and 2 C show that the errors are mainly concentrated in the end of discharge and the static process. Usually in the process of constant current charging and discharging with cut-off voltage protection, the greater the current, the smaller the amount of electricity to charge in or out theoretically, which the simulation results in this diagram can well reflect. But in actual test, the discharge capacity of these three experiments is very close, leading to obvious ‘hysteresis’ in the simulation curves of 1 C, 1.5 C, and 2 C. In addition, as battery voltage is related to SOC, the SOC of the three groups are approximately equal at the end of discharge, therefore, the final voltages are basically the same during the static setting. However, in the simulation, the discharge capacity of 1 C, 1.5 C, and 2 C decreases in turn, thus the static voltage will increase successively with the more obvious error. And the average errors in

discharge stage are 0.0156 V, 0.0146 V, and 0.0216 V, respectively, the maximum deviation is not up to 0.1 V. The final static voltage deviations are 0.149 V, 0.248 V, and 0.26 V.

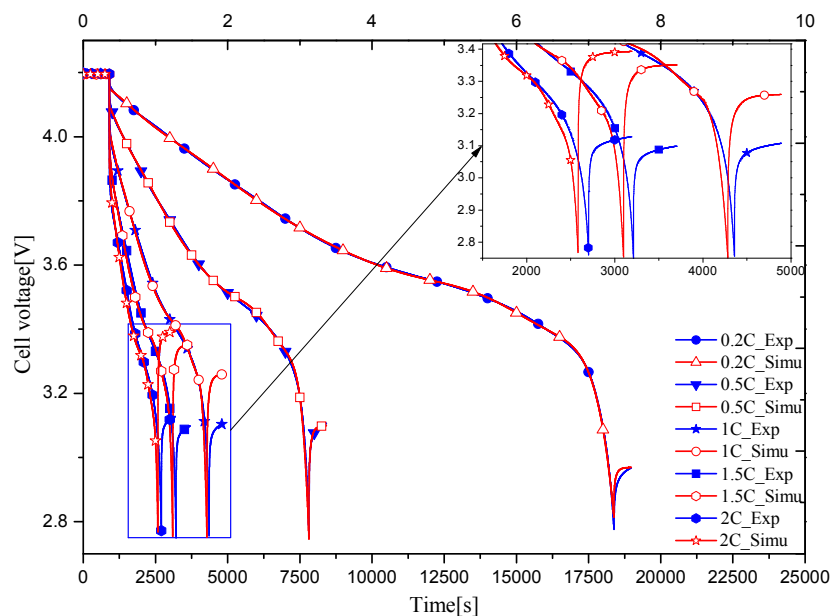


**Figure 10.** Comparison of experiment and Simulation of 0.2 C to 2 C discharge.

For further research, the effectiveness of the model parameters obtained by this identification method under actual conditions, the road simulation experiment of NEDC urban cycle condition on micro electric vehicle carried out by using chassis dynamometer. The experimental platform is depicted in Figure 11. In this experiment, the chassis dynamometer is used to simulate the road, and the two front wheel-motor controllers on the drum are given a control signal to drive the prototype car. The voltage, current, and temperature of the cell in battery management system (BMS) are collected by Controller Area Network (CAN). The car is designed with a maximum speed of 96 km/h, and its specific driving conditions as shown in Figure 12. Besides, the prototype car is also equipped with a braking energy recovery system, the battery is in a state of continuous charge and discharge during operation. The initial SOC is 100%, and is 93% at the end.



**Figure 11.** Road simulation test.

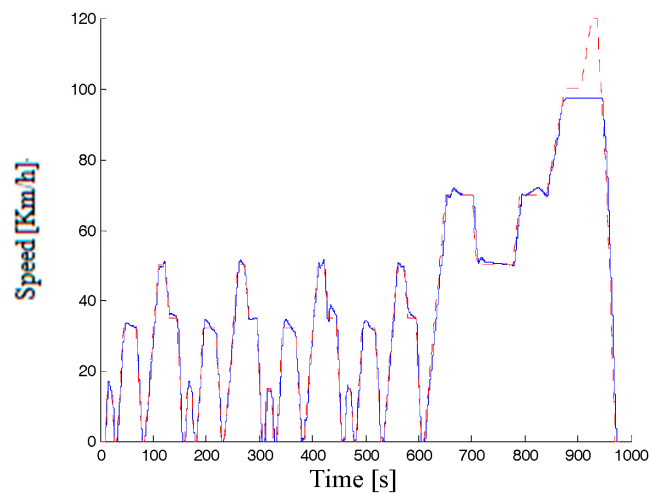


**Figure 12.** Actual speed under NEDC cycle condition.

The connection modes of cell in the battery pack are first 24 parallel connections and then 20 groups in series, and the rated voltage of pack is 82 V, the rated capacity is 127 Ah. Among them, the cell voltage can be obtained through the CAN packet, and then divide bus current by 24 to get the cell current. Finally, the simulation and experimental results are plotted in Figure 13, the charge and discharge current is small, about 0.5 C at low speed condition in city. In acceleration and at high speed condition, discharge rate can reach 1 C to 1.5 C. I found that the overall trends of these two are consistent, and really close at low speed by comparing the model output voltage with the cell voltage collected in the actual Battery Management System (BMS). The error is about  $\pm 0.03$  V. In high speed condition, the error is larger, basically about  $\pm 0.08$  V, and the maximum error can reach 0.2 V. There are two main reasons resulting in voltage error, the measurement error caused by low measuring accuracy of sensor, and the electrochemical model error proposed in this paper. The model accuracy needs to be improved when charging and discharging at high current. Furthermore, the charge and discharge efficiency, temperature, and capacity attenuation will also cause a certain deviation between the simulation and actual value, which deserve further study.

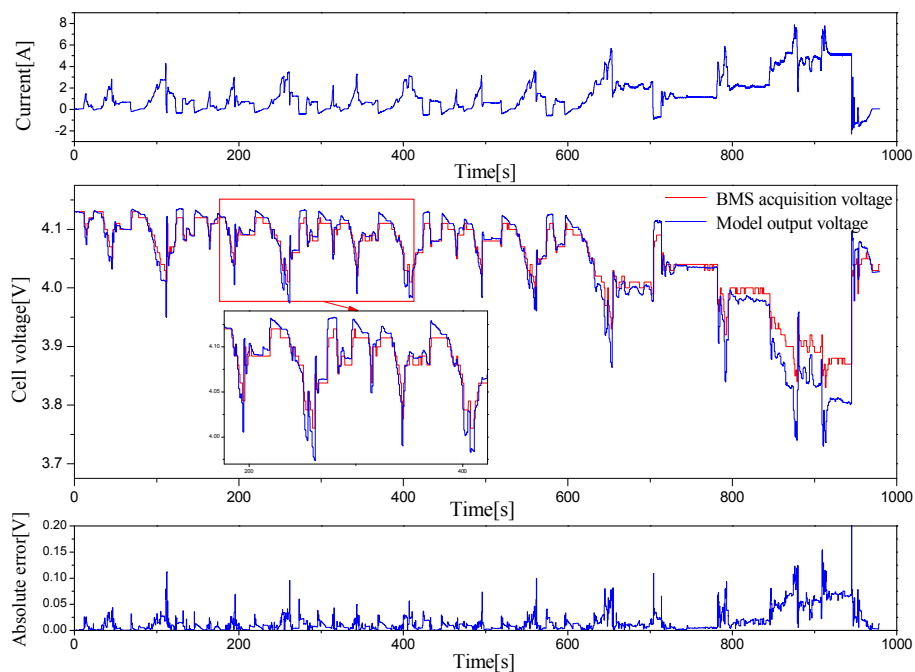


**Figure 13.** Comparison of model output voltage and actual measured value under NEDC condition.

## 5. Conclusions

In this paper, the electrode dynamics of Li ion battery is analyzed, and then the electrochemical model is established by relevant theories. The electrochemical model of the battery is a multi-loop and strongly nonlinear system. In the light of the average electrode in [15–17], the simplified average electrode model is finally built by combining the discrete finite difference method. Through the analysis and classification of the parameters, applying the particle swarm optimization (PSO) algorithm, based on the discharge experiment of 0.5 C, after two times identification, all parameters of the model are obtained with the error within its reasonable range. By the 0.2–2 C multi-rate battery discharge experiment, the parameters on the identification of particle swarm optimization algorithm can ensure the accuracy of battery model, maximum voltage error is less than 0.1 V, and only occurs in the end of large current discharge. For promoting the application of cell electrochemical models in vehicle-used battery management systems, the average electrode model put forward in this thesis, the perfection of model simplification, and the output characteristics under different working conditions are the focus of the next research.

**Acknowledgments:** This work was supported by the National Key R&D Plan of China (No. 2017YFB0103200), the National Natural Science Foundation of China (Grant No. U1664258 and U1564201), the “333” Project of Jiangsu Province (No. BRA2016445), and the Primary Research&Development Plan of Jiangsu Province (No. BE2017129).

**Author Contributions:** Xiao Yang, Long Chen and Xing Xu conceived and designed the experiments; Xiao Yang and Wei Wang performed the experiments; Xiao Yang, Wei Wang and Qiling Xu analyzed the data; Zhiguang Zhou provided equipment, technology and financial support; Xiao Yang wrote the paper; Yuzhen Lin helped and modified translation.

**Conflicts of Interest:** The authors declare no conflict of interest.

## References

1. Johnson, V.H. Battery performance models in ADVISOR. *J. Power Sources* **2002**, *110*, 321–329. [[CrossRef](#)]
2. Salameh, Z.M.; Casacca, M.A.; Lynch, W.A. A mathematical model for lead-acid batteries. *IEEE Trans. Energy Convers.* **1992**, *7*, 93–97. [[CrossRef](#)]
3. United States Idaho National Engineering & Environmental Laboratory. PNGV Battery Test Manual. Revision 3, DOE/ID-10597. 2001. Available online: [http://avtinlgov/energy\\_storage\\_lib.shtml](http://avtinlgov/energy_storage_lib.shtml) (accessed on 31 October 2017).
4. Gao, Z.; Cheng, S.C.; Chiew, J.H.K.; Jia, J.; Zhang, C. Design and Implementation of Smart Lithium-ion Battery System with Real-time Fault Diagnosis Capability for Electric Vehicles. *Energies* **2017**, *1*, 1503. [[CrossRef](#)]
5. Gao, Z.; Cheng, C.; Woo, W.; Jia, J. Integrated Equivalent Circuit and Thermal Model for Simulation of Temperature-Dependent LiFePO<sub>4</sub> Battery in Actual Embedded Application. *Energies* **2017**, *10*, 85. [[CrossRef](#)]
6. Newman, J.; Tiedemann, W. Porous-Electrode Theory with Battery Applications. *AIChE J.* **1975**, *21*, 25–41. [[CrossRef](#)]
7. Doyle, M.; Fuller, T.F.; Newman, J. Modeling of Galvanostatic Charge and Discharge of the Lithium/Polymer/Insertion Cell. *J. Electrochem. Soc.* **1993**, *140*, 1526–1533. [[CrossRef](#)]
8. Wang, C.Y.; Gu, W.B.; Liaw, B.Y. Micro-Macroscopic Coupled Modeling of Batteries and Fuel Cells. Part I: Model Development. *J. Electrochem. Soc.* **1998**, *145*, 3407–3417. [[CrossRef](#)]
9. Barbarisi, O.; Vasca, F.; Glielmo, L. State of Charge Kalman Filter Estimator for Automotive Batteries. *Control Eng. Pract.* **2006**, *14*, 267–275. [[CrossRef](#)]
10. Santhanagopalan, S.; White, R.E. Online Estimation of the State of Charge of a Lithium Ion Cell. *ECS Trans.* **1985**, *19*, 57–58.
11. Wang, C.Y.; Gu, W.B.; Liaw, B.Y. Micro-Macroscopic Coupled Modeling of Batteries and Fuel Cells. Part II: Application to Ni-Cd and Ni-MH Cells. *J. Electrochem. Soc.* **1998**, *145*, 3418–3427. [[CrossRef](#)]
12. Gu, W.B.; Wang, C.Y. Thermal-Electrochemical Coupled Modeling of a Lithium-Ion Cell. *J. Electrochem. Soc.* **2000**, *99*, 743–762.
13. Chaturvedi, N.A.; Klein, R.; Christensen, J.; Ahmed, J.; Kojic, A. Algorithms for advanced battery-management systems. *IEEE Control Syst.* **2010**, *30*, 49–68. [[CrossRef](#)]

14. Di Domenico, D.; Stefanopoulou, A.; Fiengo, G. Lithium-Ion Battery State of Charge and Critical Surface Charge Estimation Using an Electrochemical Model-Based Extended Kalman Filter. *J. Dyn. Syst. Meas. Control* **2010**, *132*, 768–778. [[CrossRef](#)]
15. Di Domenico, D.; Fiengo, G.; Stefanopoulou, A. Lithium-ion battery state of charge estimation with a Kalman filter based on a electrochemical model. In Proceedings of the IEEE International Conference on Control Applications, San Antonio, TX, USA, 3–5 September 2008; pp. 702–707.
16. Smith, K.A.; Rahn, C.D.; Wang, C.Y. Model order reduction of 1D diffusion systems via residue grouping. *J. Dyn. Syst. Meas. Control* **2008**, *130*, 141–148. [[CrossRef](#)]
17. Lee, T.K.; Filipi, Z.S. Electrochemical Li-ion battery modeling for control design with optimal uneven discretization. In Proceedings of the ASME Dynamic Systems & Control Conference & Bath/ASME Symposium on Fluid Power & Motion Control, Arlington, VA, USA, 31 October–2 November 2011; pp. 493–500.
18. Manzie, C.; Zou, C.; Netic, D. Simplification techniques for PDE-based Li-ion battery models. In Proceedings of the IEEE Conference on Decision & Control, Osaka, Japan, 15–18 December 2015; pp. 3913–3921.
19. Zou, C.; Manzie, C.; Netic, D. A Framework for Simplification of PDE-Based Lithium-Ion Battery Models. *IEEE Trans. Control Syst. Technol.* **2016**, *24*, 1594–1609. [[CrossRef](#)]
20. Wei, X.Z.; Sun, Z.C.; Tian, J.Q. Parameter identification and state estimation of Li-ion power battery in hybrid electric vehicle. *J. Tongji Univ.* **2008**, *36*, 231–235.
21. Luo, Y.T.; Xie, B.; He, X.C. Parameter identification and SOC estimation of lithium-ion battery pack used in electric vehicles. *J. South China Univ. Technol.* **2012**, *40*, 79–85.
22. Niu, L.Y.; Shi, W.; Jiang, J.C.; Zhang, Y.R.; Jiang, J.; Cao, X.M. Model parameters analysis of lithium iron phosphate battery for electric vehicle. *Automot. Eng.* **2013**, *35*, 127–132.
23. Eberhart, R.; Kennedy, J. New optimizer using particle swarm theory. In Proceedings of the International Symposium on Micro Machine and Human Science, Nagoya, Japan, 4–6 October 1995; pp. 39–43.



© 2017 by the authors. Licensee MDPI, Basel, Switzerland. This article is an open access article distributed under the terms and conditions of the Creative Commons Attribution (CC BY) license (<http://creativecommons.org/licenses/by/4.0/>).